Neuron, Vol. 22, 571–580, March, 1999, Copyright ©1999 by Cell Press

Architecture of a K^+ Channel Inner Pore Revealed by Stoichiometric Covalent Modification

Tao Lu, Bao Nguyen, Xinmin Zhang, and Jian Yang*
Department of Biological Sciences
Columbia University
New York, New York 10027

Summary

Inwardly rectifying K^+ channels bind intracellular magnesium and polyamines to generate inward rectification. We have examined the architecture of the inner pore of Kir2.1 channels by covalently attaching a constrained number (from one to four) of positively charged moieties of different sizes to the channel. Our results indicate that the inner pore is formed solely by the second transmembrane segment and is unprecedentedly wide. At a position critical for inward rectification (D172), the pore is sufficiently wide to bind three Mg^{2+} ions or polyamine molecules simultaneously. Single-channel recordings directly demonstrate that partially modified channels exhibit distinct subconductance levels. Such a wide inner pore may greatly facilitate ion permeation and high-affinity binding of multiple pore blockers to generate strong inward rectification.

Introduction

Potassium channels selectively conduct K^+ ions across cell membranes and regulate diverse biological functions (Hille, 1992). They constitute a large family of proteins that include voltage-gated K^+ (Kv) channels and inwardly rectifying K^+ (Kir) channels (Jan and Jan, 1997). Kir channels conduct current more efficiently when the membrane potential is negative to the K^+ equilibrium potential (E_K) than when positive to E_K (Hagiwara et al., 1976). This inward rectification underlies the function of Kir channels and is produced by voltage- and external K^+–dependent block of the channel by intracellular Mg^{2+} (Matsuda et al., 1987; Vandenberg, 1987; Matsuda, 1988; Ishihara et al., 1989; Lu and MacKinnon, 1994; Nichols et al., 1994; Stanfield et al., 1994; Taglialatela et al., 1994) and polyamines (Ficker et al., 1994; Lopatin et al., 1994; Fakler et al., 1995). Recent studies have identified two negatively charged residues (D172 and E224C) as key binding determinants (Ficker et al., 1994; Lopatin et al., 1994; Stanfield et al., 1994; Taglialatela et al., 1995; Yang et al., 1995a). However, it still remains unclear as to what the unique features of Kir channels are that enable them to bind cytoplasmic Mg^{2+} and polyamines. Furthermore, despite the functional importance of the inner pore in Kir channels as well as in Kv channels, where it is involved in both activation and inactivation gating (Isacoff et al., 1991; Holmgren et al., 1997; Liu et al., 1997), there is only limited information on the structure of this pore region in a vertebrate K^+ channel (Holmgren et al., 1997; Liu et al., 1997).

Kir channel subunits have two putative membrane-spanning segments (M1 and M2) and a pore-forming P loop in between (Figure 1A) (Ho et al., 1993; Kubo et al., 1993). Their transmembrane topology is identical to that of a distantly related bacterial K^+ channel, KcsA, whose three-dimensional structure has been solved recently (Doyle et al., 1998). The crystal structure of KcaA firmly establishes that four P loops—one from each of the four subunits making up the channel—extend to the center of the channel and form the external portion of the channel pore, including the K^+ selectivity filter. It also shows that the second transmembrane segment forms an inner pore consisting of a 10-Å-wide cavity in the middle of the membrane bilayer and a 6-Å-wide tunnel opening to the cytoplasm (Doyle et al., 1998). Since the P loop is conserved among all K^+ channels, it is expected to form similar structures in Kir channels. However, it remains to be determined whether Kir channels also have an inner pore similar to that of KcsA channels.

The inner pore of Kir channels is functionally important, as it harbors binding sites for intracellular Mg^{2+} and polyamines. There are indications that this pore region is particularly wide, so much so that more than one blocking molecule can bind simultaneously. First, single-channel recordings from both native and heterologously expressed Kir channels show that intracellular Mg^{2+} ions induce three distinct subconductance levels in the outward current (Matsuda, 1988; Omori et al., 1997; Oishi et al., 1998). Second, the dose–response relationship of block by Mg^{2+} and polyamines of a heterologously expressed Kir channel does not conform to one-to-one binding but instead exhibits at least two phases (Yang et al., 1995a). However, there is as yet no direct evidence that the inner pore of Kir channels is wide enough to bind multiple Mg^{2+} ions or polyamine molecules simultaneously.

In this study, we investigated the architecture of the inner pore of a strong inwardly rectifying K^+ channel (Kir2.1) (Kubo et al., 1993) by combining scanning cysteine mutagenesis and covalent chemical modification with reagents of different sizes, which were used as yardsticks to probe the pore size. We first identified residues lining the inner pore using the substituted cysteine accessibility method (SCAM) (Akabas et al., 1992), systematically mutating residues of M1 and M2 (Figure 1B) to cysteine and then probing the mutant channels with a positively charged, water-soluble sulfhydryl-specific reagent (Figure 2), which forms a covalent bond with accessible sulfhydryl groups. If the current generated by the cysteine mutant channel is irreversibly inhibited, it is inferred that the side chain of the engineered cysteine, and by extrapolation, of the original residue, is exposed to the aqueous pore. We next employed a strategy that enabled us to control the stoichiometry of the covalent modification, such that we were able to obtain singly, doubly, triply, and quadruply modified channels and hence gauge the physical dimension of the inner pore.

*To whom correspondence should be addressed (e-mail: jy160@columbia.edu).

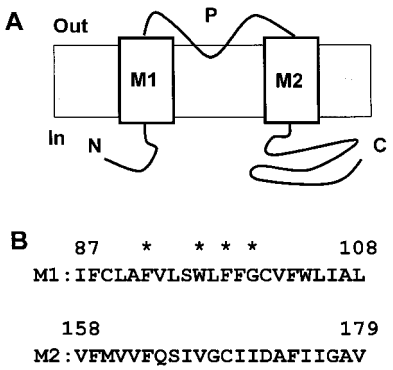

Figure 1. Schematic of a Kir Channel Subunit

(A) Putative transmembrane topology of a Kir channel subunit. Drawing is not to scale.

(B) Amino acid sequence of M1 and M2 of the Kir2.1 subunit. Single letter code is used, and the amino acid numbers are given on the top. Asterisks mark the residues that resulted in nonfunctional channels when mutated to cysteine.

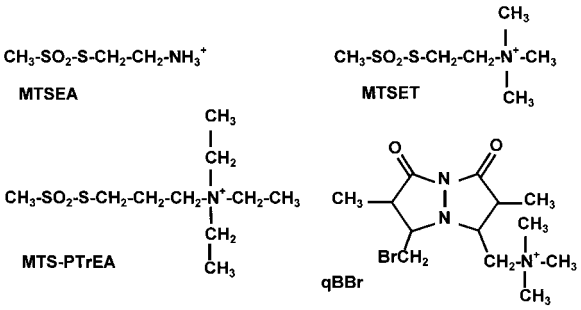

Figure 2. Chemical Structure of the Sulfhydryl-Specific Modifying Reagents Used in Our Experiments

Abbreviations: MTSEA, methanthiosulfonate- (MTS-) ethylammonium; MTSET, MTS-ethyltrimethylammonium; MTS-PTrEA, MTS-propyltriethylammonium; and qBBr, monobromotrimethyl-ammoniobimane.

Our results reveal a wide inner pore with significant implications for inward rectification and ion permeation in Kir channels.

Results

Construction of a Control Channel Nonreactive to Sulfhydryl-Specific Modifying Reagents

A prerequisite for employing SCAM is the ability to clearly distinguish the response of the cysteine mutant channels from that of wild-type channels. A difficulty we encountered at the beginning was that the wild-type Kir2.1 channel was reactive to methanthiosulfonate (MTS) reagent applied to the cytoplasmic face of the channel, including MTS-ethylammonium (MTSEA) and MTS-ethyltrimethylammonium (MTSET). As shown in Figures 3A and 3B, macroscopic current recorded in giant inside-out patches containing wild-type channels was irreversibly inhibited with a single exponential time course upon bath application of 2 mM MTSET. On average, a 2 min application of 2 mM MTSET or 2.5 mM MTSEA reduced the wild-type channel current by 93% ± 3% (n = 5) and 95% ± 2% (n = 5), respectively.

To overcome this problem, we tried to identify and mutate the reactive endogenous cysteine residues. Six of the thirteen endogenous cysteines in the wild-type subunit were mutated altogether, either to valine (C54V and C76V) or to their counterparts in the Kir1.1 subunit (Ho et al., 1993; C89I, C101L, C149F, and C169V). The resulting mutant channel, named IRK1J, was much less reactive to internal MTS reagents, as shown in Figures 3C and 3D. On average, 2 mM MTSET and 2.5 mM MTSEA produced only 7.5% ± 3.0% (n = 4) and 8.0% ± 3.2% (n = 5) irreversible current inhibition, respectively. IRK1J channels were also not reactive to extracellular MTSET, as determined by two electrode voltage-clamp (TEVC) (data not shown).

Interestingly, internal MTSET (and MTSEA) produced a reversible inhibition of the outward current through IRK1J channels, resulting in a strong inward rectification (Figure 3D). The mechanism of this inward rectification appeared to be similar to that induced by Mg^{2+} or polyamines and was not investigated further.

Because of the sextuple mutation, IRK1J channels exhibited a reduced single-channel chord conductance of 6.0 ± 0.1 pS (n = 6) at −100 mV in cell-attached patch recordings compared with 18 ± 0.7 pS (n = 7) for the wild-type channels. However, IRK1J channels behaved similarly to the wild-type channels in other aspects, including high selectivity for K^+, strong inward rectification, and high affinity for Mg^{2+} and polyamines, suggesting that the mutations did not induce significant structural changes in the pore region. Therefore, we used IRK1J as the control channel and constructed all cysteine mutations on this background.

The Inner Pore Is Formed Solely by the Second Transmembrane Segment

To determine the residues lining the inner pore, we replaced, one by one, twenty-two consecutive residues in both M1 and M2 (Figure 1B) of IRK1J subunit with a reporter cysteine. All but four mutant subunits formed functional homotetrameric channels in oocytes, and except D172C, all mutant channels retained high selectivity for K^+ as well as strong inward rectification.

We first tested the accessibility of D172C, since this acidic residue has been shown to be important for ion permeation as well as Mg^{2+} and polyamine binding (Ficker et al., 1994; Lopatin et al., 1994; Stanfield et al., 1994; Taglialatela et al., 1995; Yang et al., 1995a) and therefore is expected to project into the aqueous pore. Indeed, application of 2 mM MTSET to the cytoplasmic side of D172C channels rapidly abolished the current (Figures 4A and 4B). This inhibition was irreversible after washout of MTSET, indicating that it was due to covalent modification of the channels by MTSET. This conclusion was further tested with 1,4-dithiothreitol (DTT), a reducing reagent that breaks disulfide linkages. As shown in Figure 4B, the complete current inhibition induced by internal MTSET could be completely reversed by the internal application of 50 mM DTT, which by itself had a reversible inhibitory effect on the channel.

Figure 4C summarizes the effects of internal MTSEA

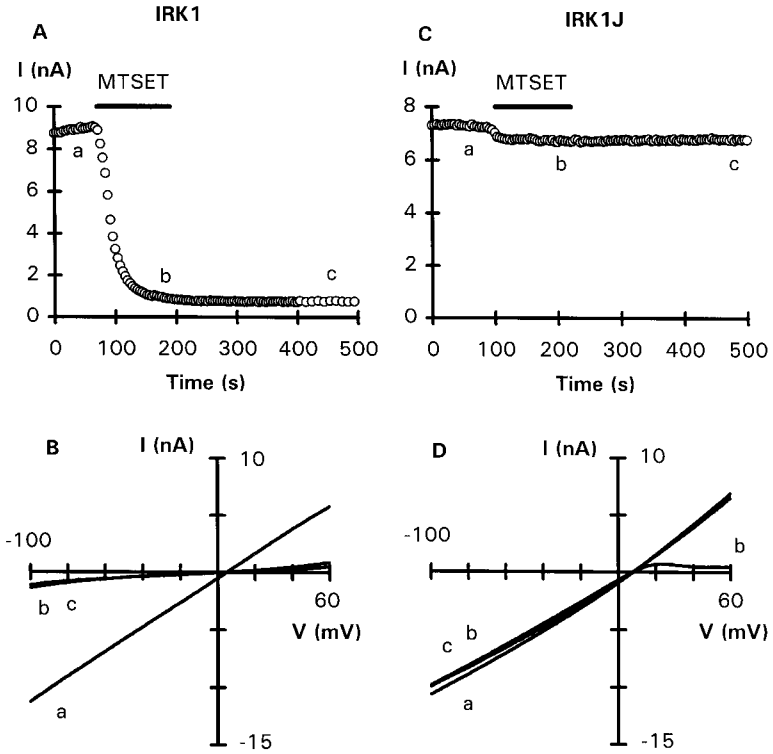

Figure 3. A Control Channel Not Reactive to Sulfhydryl-Specific Reagents

(A and B) Effect of internal MTSET on wild-type Kir2.1 channels.

(C and D) Effect of internal MTSET on the control IRK1J channels.

(A and C) Time course of inhibition of inward current (sign reversed) at −80 mV by internal MTSET. Current was sampled at 4 or 10 s intervals.

(B and D) Current–voltage (I–V) relations from the corresponding patch, before (a), during (b), and after (c) MTSET application. Current was generated by voltage ramps from −100 mV to +80 mV over 70 ms. Notice in (D) that the I–V relation obtained in the presence of MTSET exhibits strong inward rectification (b), which is reversible after washout of MTSET (c).

and MTSET (head group diameter, 3.6 Å and 5.8 Å, respectively) on the M2 cysteine mutant channels. Eight of the twenty-two mutant channels showed varying degrees of irreversible block by MTSEA or MTSET. The side chain of these residues is presumably exposed to the aqueous pore. Table 1 shows the apparent second-order rate constant of modification at a holding potential of −40 mV, obtained by fitting the time course of current inhibition with a single exponential function. MTSEA reacted faster than MTSET in all cases. However, the reaction rate with all mutant channels, including D172C, is much slower than the reported 40,000–90,000 M^{-1} s^{-1} reaction rate with 2-mercaptoethanol (Stauffer and Karlin, 1994). Strikingly, none of the 18 functional M1 mutant

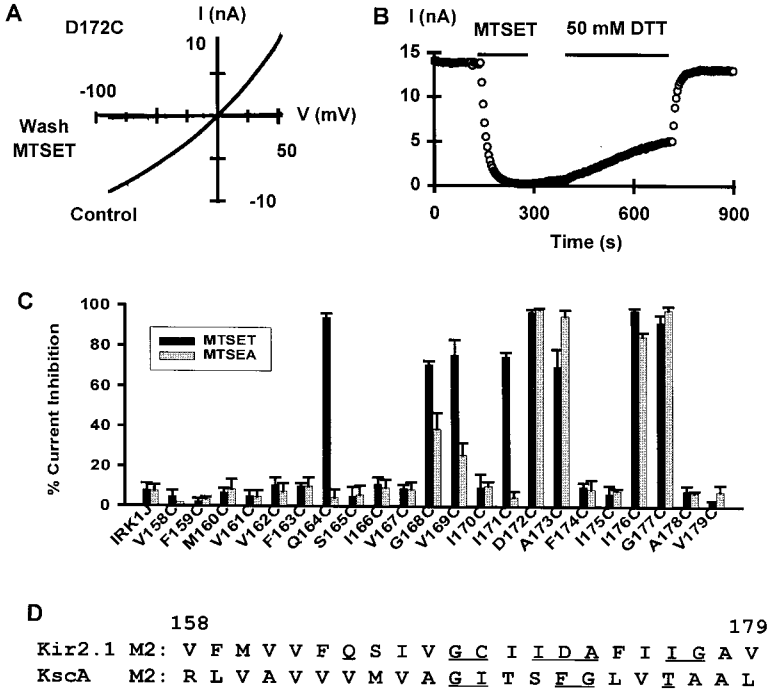

Figure 4. Determination of Amino Acid Residues Lining the Inner Pore

(A) I–V relations of D172C channels before, during, and after internal MTSET treatment.

(B) Time course of inhibition of inward current (sign reversed) at −80 mV by MTSET and subsequent reversal after application of 50 mM DTT to the intracellular side of an inside-out patch. Current was sampled at 4 s intervals.

(C) Inhibition of current at −80 mV by internal MTSEA or MTSET on IRK1J and M2 cysteine mutant channels (n = 3–6). Steady-state effect was achieved for all channels with the exception of MTSET modification of A173C, which did not reach steady state in 8 min.

(D) Sequence alignment of M2 of Kir2.1 and KcsA. The underlined amino acids are pore-lining residues.

Table 1. Apparent Second-Order Rate Constant of MTSEA and MTSET Reactions with Cysteine Residues in M2

	Q164C	G168C	V169C	I171C	D172C	A173C	I176C	G177C
MTSEA	ND	22 ± 3	11 ± 4	ND	164 ± 8	5 ± 2	111 ± 20	44 ± 9
MTSET	8.8 ± 1	1.1 ± 0.3	6.5 ± 2	2.2 ± 1	18 ± 5	ND	33 ± 8	7 ± 2

The rate constants are in $M^{-1}S^{-1}$ and were obtained at a holding potential of −40 mV. Two-and-a-half millimolars MTSEA or 2 mM MTSET was applied to the intracellular side of giant inside-out patches containing the mutant channels for 2–8 min, depending on the reaction rate to reach the steady-state effect. Only reactive channels are shown. The apparent second-order rate constant was calculated as described in Experimental Procedures. Abbreviation: ND, not determined. Data are presented as mean ± SD (n = 3–6).

channels were reactive to either MTSEA or MTSET—their responses were indistinguishable from that of IRK1J (data not shown). These results indicate that the inner pore of Kir2.1 channel is lined solely by residues from M2. This conclusion is in good agreement with the X-ray structure of KcsA (Doyle et al., 1998). However, two differences exist between the two channels. First, besides the counterpart of the four M2 pore-lining residues found in KcsA, four additional residues were found to line the Kir2.1 inner pore (Figures 4C and 4D). One of them, Q164, is positioned two-thirds of the way into the membrane bilayer from the inside, indicating that the pore region formed by M2 extends from the inner surface beyond the center of the membrane. Second, as shown in Figures 4C and 4D, five of six consecutive residues (G168–A173) in the M2 segment of Kir2.1 were found to point to the pore. This side chain projection pattern is incompatible with a continuous α-helical structure, as shown for KcsA.

A Wide Pore Revealed by Stoichiometric Covalent Modification at Position D172

Kir channels are composed of four subunits (Glowatzki et al., 1995; Yang et al., 1995b), like Kv and KcsA channels (MacKinnon, 1994; Doyle et al., 1998). Thus, a reactive homomeric mutant channel contains four identical modifiable cysteine residues. Is modification of one subunit sufficient, or must all four subunits be modified to produce complete current inhibition? To address this question, we employed a strategy that would allow us to control the stoichiometry of the covalent modification by concatenating varying numbers of IRK1J and cysteine mutant subunits into a tandem tetramer. Studies have shown that four K^+ channel subunits linked in a single protein chain can preferentially coassemble to form functional channels identical to those formed by four monomeric subunits (Liman et al., 1992; Yang et al., 1995b). Given its functional importance, we again focused on position D172. Figure 5A displays the effect of internal MTSET on channels containing from zero to four D172C subunits. Remarkably, the singly, doubly, and even triply modified channels could still conduct K^+ current, and there was a striking correlation between the magnitude of current inhibition and the number of modified subunits in the channel. The current was blocked by 24% ± 1.0% (n = 3), 55% ± 4.0% (n = 4), 80% ± 0.6% (n = 3), and 97% ± 1.0% (n = 3), respectively, for channels containing from one to four D172C subunits. The partial inhibition of channels containing from one to three D172C subunits was not due to the slow reaction rate of MTSET, since steady-state block was achieved in all cases (Figures 5B and 5C and Table 2). Thus, all four subunits must be modified by MTSET to completely occlude K^+ flow through the pore, indicating that the pore region harboring D172 (which is positioned one-third of the way into the membrane bilayer from the inside) is wide enough to simultaneously accommodate four -S-CH_2-CH_2-N$(CH_3)_3^+$ groups.

Such a wide pore may also exist at several other positions, including Q164, G168, V169, and I171, since the homomeric channels carrying cysteine mutations at these positions could still conduct significant K^+ current after modification by MTSEA or MTSET (Figure 4C). In this regard, it is interesting to note that two of the reactive mutant channels, Q164C and I171C, were inhibited by MTSET but not by MTSEA (Figure 4C). For both mutant channels, however, pretreatment of MTSEA prevented subsequent inhibition by MTSET (data not shown), indicating that MTSEA did form a covalent linkage with the engineered cysteines in the mutant channels and hence prevented them from subsequent reaction with MTSET, but the covalent modification did not affect ion conduction. These results suggest that the pore lined by these residues is indeed wide, to the extent that K^+ conduction is virtually unaffected even after one or more of the four subunits making up the channel are covalently modified by MTSEA.

Channels Partially Modified by MTSET Show Subconductance Levels

The stepwise reduction of the macroscopic current (Figure 5A) suggests that channels partially modified by MTSET can still conduct current and thus may exhibit subconductance levels. To test this hypothesis, we examined at the single-channel level modification by MTSET of channels carrying one or two D172C subunits. Representative single-channel records (Figures 6Aa and 6Ba) from inside-out patches and the corresponding amplitude histograms (Figures 6Ab and 6Bb) clearly show two distinct subconductance levels after covalent modification by internal MTSET. As expected, modification of two subunits resulted in a more severe effect than of one. The chord conductance at −140 mV before and after MTSET modification was 6.6 ± 0.4 pS and 4.8 ± 0.2 pS (n = 5) for channels containing one D172C subunit and 7.0 ± 0.9 pS and 3.2 ± 0.6 pS (n = 5) for channels containing two D172C subunits, a reduction of 27% and 54%, respectively (Figures 6Ac and 6Bc). We also attempted to examine modification of single channels containing three D172C subunits, but the much reduced current after MTSET modification prevented an unambiguous identification of the channel openings. Nonetheless, the single-channel results from the singly and doubly modified channels match remarkably well

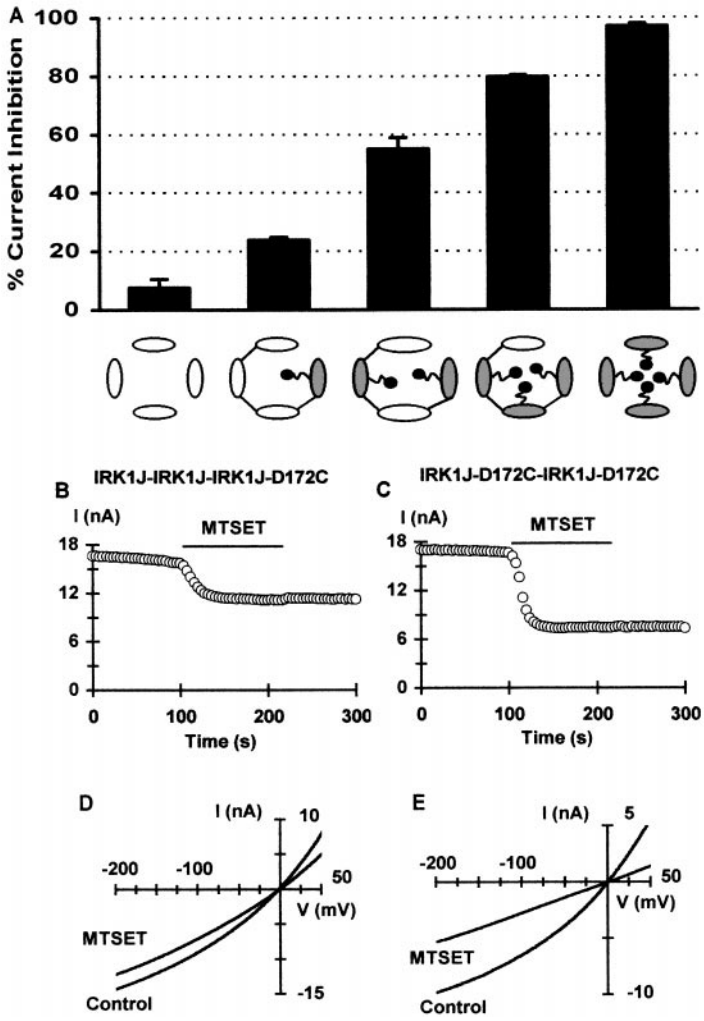

Figure 5. Stepwise Block by MTSET of Channels Containing a Constrained Number of Modifiable Subunits

(A) Steady-state inhibition of macroscopic current at −80 mV by internal MTSET in channels containing from zero to four D172C subunits (depicted by the cartoons).

(B and C) Time course of inhibition of inward current (sign reversed) at −80 mV by internal MTSET in channels containing one or two D172C subunits. Current was sampled at 4 s intervals.

(D and E) I–V relations of channels containing one or two D172C subunits before and after modification by internal MTSET.

those obtained from the macropatch recordings (Figure 5A) and directly confirm that multiple -S-CH_2-CH_2-$N(CH_3)_3^+$ groups from MTSET can indeed be accommodated in a single pore.

The Inner Pore Is Unprecedentedly Wide

To further explore the physical dimension of the pore at position D172, we examined covalent modification of the same set of channels as in Figure 5A by three

Table 2. Inhibition of Channels Containing 1–4 D172C or I176C Mutant Subunits by Sulfhydryl-Specific Modifying Reagents

	MTSEA (2.5 mM)	MTSET (2 mM)	MTS-PTrEA (4 mM)	qBBr (4 mM)
IRK1J	8.0 ± 3.2 (5)	7.5 ± 3 (4)	8.7 ± 3 (3)	6 ± 5 (5)
1 D172C	25 ± 3 (4)	24 ± 1 (3)	35 ± 1.2 (3)	34 ± 1.1 (3)
2 D172C	49 ± 5 (4)	55 ± 4 (4)	72 ± 1.5 (3)	70 ± 1.5 (3)
3 D172C	71 ± 2 (4)	80 ± 0.6 (3)	83 ± 2 (4)	81 ± 1.5 (3)
4 D172C	98 ± 1 (3)	97 ± 1 (3)	85 ± 3 (5)*	85 ± 3.8 (3)*
1 I176C	18 ± 1.5 (4)	51 ± 3 (4)	54 ± 6 (3)	59 ± 5 (3)
2 I176C	32 ± 3 (5)	80 ± 4 (6)	90 ± 2.7 (3)	93 ± 1 (3)
3 I176C	57 ± 2.6 (4)	89 ± 1.5 (4)	92 ± 2 (3)	93 ± 1 (3)
4 I176C	79 ± 6 (10)	98 ± 0.6 (3)	97 ± 1 (3)	95 ± 0.6 (3)

Data represent steady-state percentage inhibition of macroscopic current at − 80 mV. The reagent was applied to the intracellular side of a giant inside-out patch for 2–8 min, depending on the reaction rate to reach the steady-state effect. For MTSET, MTSPT, and qBBr, the steady-state modification was confirmed by the lack of further inhibition upon subsequent treatment with MTSEA, which had the fastest reaction rate ($\tau < 10$ s in all cases). Asterisks mark the only two exceptions in which MTSEA caused a complete inhibition following such a protocol. Percentage inhibition was calculated as described in Experimental Procedures. Data are presented as mean ± SD (number of observations). Pair wise comparison indicates that first, the responses of channels containing 1–4 mutant subunits to MTSEA or MTSET are significantly different from each other ($p < 0.005$) at both positions, and second, the response to MTSPT or qBBr of channels containing 1–3 D172C subunits and that of channels containing 1 or 2 I176C subunits are significantly different from each other ($p < 0.005$).

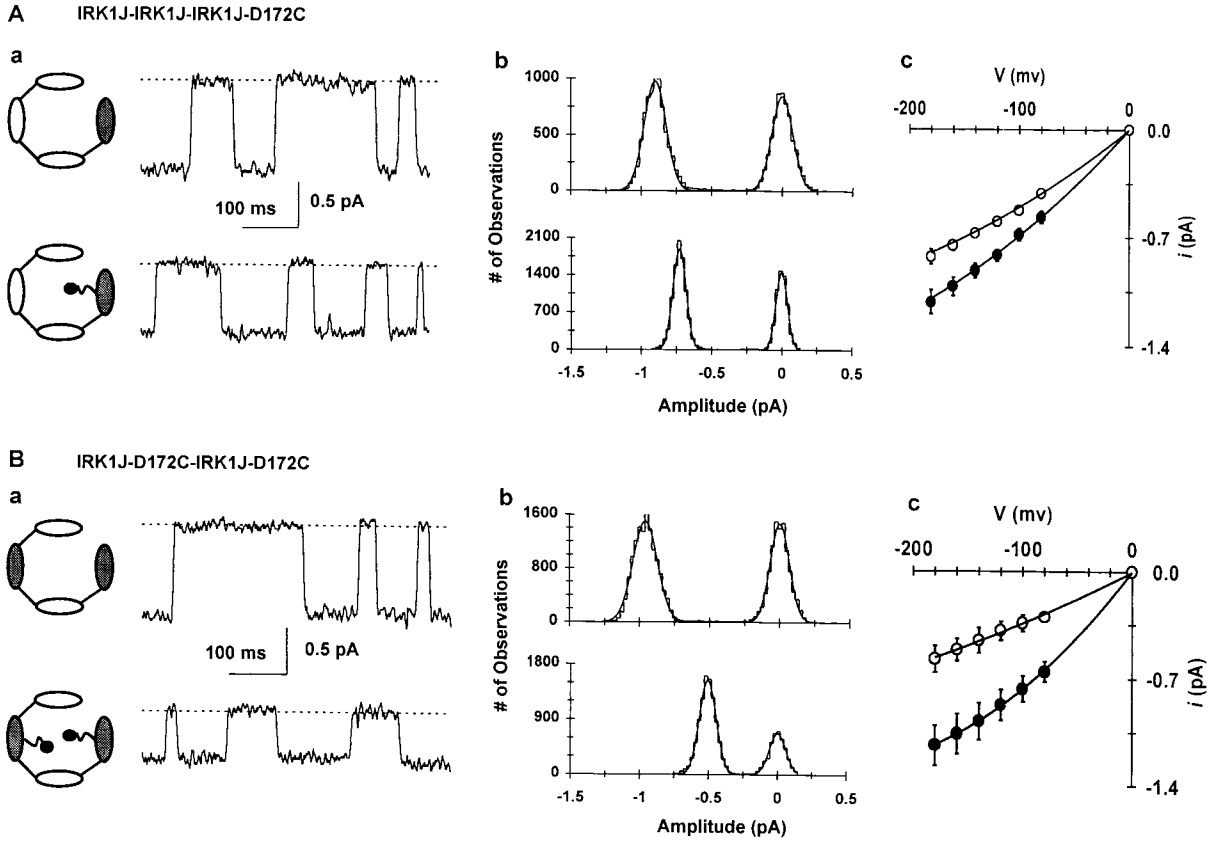

Figure 6. Single-Channel Subconductance Levels Induced by MTSET Modification

(Aa and Ba) Single-channel currents at −140 mV before and after modification by internal MTSET of channels containing one (A) or two (B) D172C subunits. Dashed lines indicate closed state.

(Ab and Bb) Amplitude histograms at −140 mV from the corresponding patches. Smooth lines are Gaussian fits.

(Ac and Bc) Single-channel I–V relations before (closed circles) and after (open circles) modification by MTSET. Lines are fits to a second-order polynomial intersecting the origin, showing similar outward rectification, as seen in macropatches (Figures 5D and 5E).

additional positively charged thiol-specific reagents: MTSEA, MTS-propyltriethylammonium (MTS-PTrEA), and monobromotrimethyl-ammoniobimane (qBBr) (Kosower et al., 1979). MTSEA has a head group of 3.6 Å and has the fastest reaction rate. On the other hand, the attaching moiety of MTS-PTrEA has a large head group similar to that of tetraethylammonium (∼8 Å in diameter), a classic K^+ channel blocker, and the head group of qBBr is even bulkier (with dimensions of >12 Å × 10 Å × 6 Å) and more rigid (Figure 2). These reagents, together with MTSET, allowed us to systematically gauge the pore size.

Table 2 and Figure 7A summarize the effect of these reagents on channels containing from zero to four D172C subunits. For all four reagents, there is a general correlation between the magnitude of current inhibition and the number of modified subunits in the channel. Clearly, MTSEA and MTSET must modify all four subunits to block the channel completely. As expected, MTS-PTrEA and qBBr produced more inhibition than MTSEA in channels containing 1–3 D172C subunits. But the singly, doubly, and triply modified channels were not completely blocked. Interestingly, MTS-PTrEA and qBBr also failed to completely block the homotetrameric D172C channels even though the much smaller MTSEA did. Instead, they produced inhibition similar to that in channels containing three D172C subunits. These results indicate that three and only three MTS-PTrEA or qBBr moieties can be accommodated in this pore region and that the triply modified pore is still wide enough to permit K^+ flow. The remaining unmodified cysteine residue at position D172 was still accessible to MTSEA, since subsequent application of MTSEA resulted in a complete block of the channel (Figure 7A, asterisk). These results, taken together, indicate that the pore region harboring D172 is sufficiently wide to simultaneously accommodate three 8- to 10-Å-wide moieities plus one 3.6-Å-wide moiety.

How do MTS-PTrEA and qBBr reach a position as deep in the pore as D172—by diffusion through the inner pore or through the membrane lipid? To address this question, we tested the effect of both reagents on the homomeric D172C channel from the extracellular side. Application of 2 mM MTS-PTrEA or 4 mM qBBr over 40 min had no effect on the whole-cell current recorded by TEVC (data not shown), suggesting that they are membrane impermeant. Thus, these molecules must travel through the entire length of an inner pore wider than their diameter (>8–10 Å). This notion is further supported by the covalent modification results (Figure 7B)

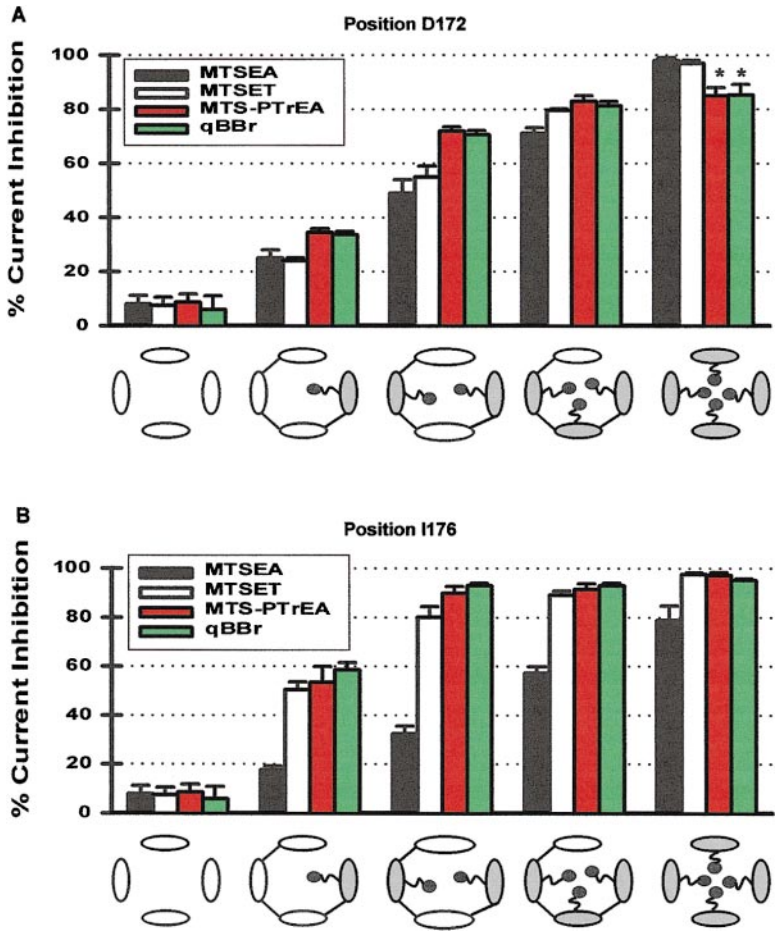

Figure 7. A Wide Inner Pore Revealed by Stoichiometric Covalent Modification at Two Different Positions

Steady-state inhibition of macroscopic current at −80 mV by MTSEA, MTSET, MTS-PTrEA, and qBBr in channels containing from zero to four D172C subunits (A) or I176C subunits (B) (n = 3–6). Asterisks in (A) mark the only two cases in which subsequent application of MTSEA caused further and complete inhibition.

at another locus, I176, located closer to the inner surface of the membrane. Unlike D172, the pore at I176 can accommodate only two instead of three MTSPT or qBBr moieties, since the doubly modified channel was nearly fully blocked. Thus, the pore appears narrower at position I176 than at D172. However, this pore region is still wide enough to hold four MTSET moieties and, surprisingly, to permit K^+ conduction even after all four subunits are modified by MTSEA.

Discussion

The inner pore of Kir channels binds intracellular Mg^{2+} and polyamines to produce inward rectification. The molecular architecture of this functionally important pore region was investigated in this study by SCAM (Akabas et al., 1992) and by covalently attaching a constrained number of positively charged moieties of different sizes at two key positions in the inner pore. Our results lead us to conclude that the second transmembrane segment of Kir2.1 forms an unprecedentedly wide inner pore that is capable of binding multiple Mg^{2+} ions and polyamine molecules simultaneously.

Architecture of the Inner Pore of Kir2.1 Channels

SCAM has been used to determine pore-lining residues in a number of voltage- and ligand-gated ion channels (reviewed by Karlin and Akabas, 1998). A key assumption is that the cysteine residues that are accessible to charged, hydrophilic, and sulfhydryl-specific reagents project into and line the aqueous pore. Our present results show that SCAM has remarkable specificity when applied to the membrane-spanning regions of Kir2.1. First, none of the 18 tested positions in M1 were accessible to MTSEA or MTSET, in agreement with the crystal structure of KcsA (Doyle et al., 1998), which clearly shows that M1 is positioned behind M2 and facing the membrane lipid. Second, the four pore-lining residues identified in the M2 of KcsA by crystallography were also identified by SCAM in the M2 of Kir2.1 (Figure 4D). These results, although they do not prove the validity of the assumption mentioned above, provide confidence for the use of SCAM in our study.

Interpretation of our results obtained from the tandem tetramers depends critically on their proper assembly. It has been shown that channels expressed from Kir2.1 tandem tetramers are formed predominantly by the intramolecular assembly of the tetramers, with occasional intermolecular association of two or more tetramers (Yang et al., 1995b). To ascertain that the tandem tetramers used in our current study assembled properly, we created a tandem tetramer that contained three IRK1J subunits and one mutant subunit in which G144, Y145, G146, and R148 in the P loop were replaced simultaneously with alanine. Our rationale was that the quadruple mutation in the ion selectivity filter would produce a dominant-negative effect and hence render the channels that were properly formed by the tetramers noncon-

ducting. Any residual current generated by the tandem tetramer must then come from the intermolecular assembly of two or more tetramers. We found that upon expression in oocyte with an equal amount of RNA, the mutant tetramer only generated <5% of the current compared with that produced by the wild-type tetramer (data not shown), indicating that indeed ~95% of the mutant tetramers assembled properly. In strong support of this conclusion, we observed that the magnitude of current inhibition produced by MTSET modification was nearly identical at the macroscopic and single-channel levels for channels containing one or two D172C subunits (compare Figures 5 and 6).

Our finding that four -S-CH_2-CH_2-N$(CH_3)_3^+$ moieties from MTSET (with a head group 5.8 Å wide) can be simultaneously linked to position D172 or I176 indicates that the pore at these positions is wide. Because the spatial arrangement of these covalently linked groups and nearby side chains is unknown, it is difficult to deduce a precise physical dimension of the pore. Nevertheless, even assuming that only two head groups lie side by side, the pore must be >12 Å wide. This conclusion is further supported by the modification results with qBBr (Figure 7), whose cyclic attaching moiety (with a dimension of >12 Å × 10 Å × 6 Å) is substantially larger than that of MTSET and is more rigid. A space-filling model of the entire M2 segment of Kir2.1 (assuming a helical structure) indicates that the pore regions at I176 and D172 must indeed be >12 Å wide in order to accommodate two or three modifying groups from qBBr. This estimated diameter is most likely an underestimate, considering the unfavorable steric hindrance and electrostatic repulsion among these groups. The recent observation that tetrapentylammonium, which is ~12 Å in diameter, can block Kir channels from the cytoplasmic side (Oliver et al., 1998; Spassova and Lu, 1998) is in good agreement with our finding of a >12-Å-wide inner pore.

The reaction rate of MTSEA and MTSET with reporter cysteines in M2 of Kir2.1 (Table 1) is 2–4 orders of magnitude slower than that with free thiols (Stauffer and Karlin, 1994) or with cysteine residues in S6 of a Kv channel (Liu et al., 1997). Such a slow rate appears to contradict the conclusion that the inner pore of Kir2.1 is >12 Å wide. Two factors may contribute to this paradox. First, the experiments with MTSEA and MTSET were performed at a holding potential of −40 mV, at which there was a constant inward current through the channels under study. Thus, the modifying reagents were constantly swept out of the pore by the continuous inward flux of K^+ ions, drastically lowering the effective concentration in the pore. Second, both reagents can bind as pore blockers to the inner pore to produce inward rectification (Figure 3D), and this binding may severely hamper the access to and the subsequent covalent modification of the reporter cysteines. Because of these factors, the apparent reaction rates were most likely greatly underestimated. In a few test experiments, we used a holding potential of 0 mV and did observe a dramatic increase in the rate of current inhibition. However, because of the rapid voltage-dependent block by the modifying reagents, it was difficult to accurately assess the rate of the covalent modification under such a recording condition.

Although our results do not provide definitive structural measurements, they allow us to deduce several molecular features of the inner pore of Kir2.1 channels. First, only residues in M2 form the lining of the inner pore. Second, there is a large aqueous chamber (>12 Å across) in the center of the membrane bilayer, encompassing and lined by residues Q164, G168, C169, I171, and D172. Third, the inner pore narrows somewhat toward the cytoplasmic end but is still wider than 10 Å (in order to pass MTS-PTrEA and qBBr). This part of the pore is lined by A173, I176, and G177. Many of these features are similar to those directly demonstrated by the crystal structure of the KcsA channel (Doyle et al., 1998). However, the Kir2.1 inner pore appears significantly wider. Indeed, even the narrowest part of the inner pore seems to be wider than the central cavity in KcsA. Factors such as the lipid environment, the open/closed state of the channel, and the presence/absence of cytoplasmic domains may contribute to this and other differences mentioned in the Results, but these two functionally distinct and distantly related K^+ channels may truly differ in the structure of their inner pores.

Functional Implications

A wide inner pore of >12 Å across has significant implications for inward rectification and ion permeation in Kir channels. The demonstration (Figure 7A and Table 2) of a cooccupancy of three 8- to 10-Å-wide positively charged groups plus one 3.6-Å-wide positively charged group at position D172 (after neutralization of the four negative charges) suggests not only that this pore region is physically wide enough to simultaneously bind three partially hydrated Mg^{2+} ions (<8 Å with 6 H_2O) or three vertically aligned polyamine molecules (4 Å wide and 7–18 Å long) but also that it is electrostatically plausible. Such a novel binding mechanism provides a molecular explanation for the multiphase dose–response relationship of Mg^{2+} and polyamine block of Kir2.1 channels (Yang et al., 1995a) and the strong voltage dependence of some native Kir channels with an equivalent gating charge of 2.5–6 elementary charges (Adrian, 1969; Hagiwara and Jaffe, 1979; Silver and DeCoursey, 1990).

An intriguing feature of Mg^{2+} block of Kir channels is that, at low concentrations, internal Mg^{2+} blocks the outward current in three discrete steps. These subconductance states were first recorded from a cardiac Kir channel (Matsuda, 1988) and recently from Kir2.1 channels expressed in a cell line (Omori et al., 1997; Oishi et al., 1998). (We have not been able to obtain these subconductance states in Kir2.1 channels expressed in oocyte due to technical difficulties [see Experimental Procedures].) The three equally spaced subconductance states were originally interpreted as evidence that the Kir channel consists of three identical and separate pores, each of which can be blocked independently by a single Mg^{2+} ion (Matsuda, 1988). However, our results strongly suggest an alternative mechanism—that these subconductance states are induced by the binding of three or more Mg^{2+} ions in a single wide pore. The most direct evidence supporting this type of mechanism comes from the observation that distinct subconductance levels can be induced by covalently attaching one or two MTSET moieties to Kir2.1 channels (Figure 6).

This model is also supported by the recent report that neutralization of different numbers of D172 in Kir2.1 channels affected the Mg^{2+}-induced subconductance states (Oishi et al., 1998). Distinct subconductance levels induced by protons have been observed in other ion channels as a result of the protonation of negatively charged residues at the external entrance of the pore (Root and MacKinnon, 1994; Chen et al., 1996). But to our knowledge, binding of multiple pore blockers deep in a channel pore is a novel observation.

Kir channels have traditionally been thought to have a long single-file pore (Hille and Schwarz, 1978; Lopatin et al., 1995). Our findings appear to challenge this view. The conclusion that four positively charged groups can be simultaneously accommodated in the inner pore of Kir2.1 channels suggests that ion permeation through this region may not be single file. Thus, in Kir2.1 channels, single-file ion permeation may be limited only to the external and narrowest part of the channel pore—the 12-Å-long ion selectivity filter (Doyle et al., 1998). An aqueous inner pore $>$12 Å wide extending from the cytoplasm to and beyond the center of the membrane greatly facilitates K^+ permeation, since it permits free diffusion of hydrated K^+ ions and thus diminishes the dielectric forces impeding the movement of K^+ ions across the membrane (Levitt, 1978; Jordan, 1982; Hille, 1992).

Experimental Procedures

Construction of Cysteine Mutants and Tandem Tetramers

Site-directed mutations were generated by either PCR cassette mutagenesis or the oligonucleotide insertion method and were confirmed by sequencing. All cysteine mutations were made with IRK1J subunit, which was subcloned into pGEMHE containing the 5′ and 3′ untranslated regions of a *Xenopus* β-*globin* gene as the background (Liman et al., 1992).

Tetrameric cDNAs were constructed in three steps as described previously (Yang et al., 1995b). First, four monomeric cDNAs with unique restriction site(s) and/or linkers were constructed in pBluescript SK- (Strategene). For subunit A, a linker containing ten glutamines plus the first ten amino acids from IRK1J subunit with a built-in PinAI site was ligated into the AflII–HindIII sites. For subunit B, a linker containing ten glutamines and residues Thr/Arg (bearing an MluI site) was subcloned as described above, and a PinAI site was engineered at the beginning of the N terminus at the Asn/Arg residues. For subunit C, an MluI site was created in subunit A immediately before the starting codon. Subunit D was the same as B but without the linker and carrying a cysteine mutation. Second, the PinAI–HindIII fragment from B was ligated in-frame into A to create dimer A-B, and the fragment from D was ligated in-frame into C to create dimer C-D. Third, the PstI–MluI fragment from A-B was subcloned into C-D to produce a tetrameric cDNA. The BamHI–HindIII fragment containing the entire coding region was then subcloned from pBluscript SK^- into pGEMHE. Tandem tetramers containing from one to three cysteine mutant subunits were created by linking one, two, or three mutant subunits with three, two, or one IRK1J subunit, respectively. They are designated as IRK1J-IRK1J-IRK1J-X, IRK1J-X-IRK1J-X, and IRK1J-X-X-X, where X denotes the cysteine mutant subunit. cRNAs for all constructs were transcribed in vitro with the T7 RNA polymerase following linearization of the cDNAs with NheI.

Oocyte Expression

Ovarian lobes were obtained from adult *Xenopus laevis* under anesthesia. Stages V–VI oocytes were prepared by treatment with 2.5 mg/ml collagenase A (Boehringer Mannheim) for 1.5–2.5 hr under 200 rpm shaking in a solution containing 82.4 mM NaCl, 2.5 mM KCl, 1 mM $MgCl_2$, and 5 mM HEPES (pH 7.6) and then rinsed twice (15 min each) with ND96 solution containing 96 mM NaCl, 2.5 mM KCl, 1 mM $MgCl_2$, 5 mM HEPES, 1.8 mM $CaCl_2$, 100 U/ml penicillin, and 100 μg/ml streptomycin (pH 7.6). Single, defoliculated oocytes were individually selected, injected with 0.2–5 ng of cRNA, maintained in ND96 solution in an 18°C incubator, and used for recordings 2–10 days after injection.

Electrophysiology

Patch-clamp recordings were performed with the Axopatch 200A amplifier (Axon Instruments). All recordings were performed by using the inside-out configuration. Oocyte was bathed in an Mg^{2+}- and polyamine-free control solution containing 110 mM KCl, 10 mM HEPES, 9 mM EGTA, 1 mM EDTA, 200 μM $CaCl_2$, and 200 μM KF (pH 7.3 with KOH; total K^+, ~140 mM). Recording glass pipettes pulled from pyrex glass tubes (Corning) were filled with a solution of 130 mM KCl, 10 mM HEPES, and 3 mM $MgCl_2$ (pH 7.3 with KOH; total K^+, ~140 mM) and had a resistance of 0.2–1.5 MΩ for giant macropatch recording or 6–10 MΩ for single-channel recording. Control and test solutions were fed by gravity through separate tubes to a manifold attached to a single outlet tube with a diameter of ~150 μm and were switched on/off individually. After obtaining the inside-out patches, the recording pipette was inserted into the perfusion tube to achieve a rapid and complete exchange of solution.

We have repeatedly attempted to study block of Kir2.1 single-channel outward current by Mg^{2+} and polyamines, but our effort was hampered by two technical difficulties. First, we have not been able to obtain outward single-channel current due to the extreme difficulty of washing out cytoplasmic polyamines in inside-out, single-channel patches. Second, for unknown reasons, Kir2.1 channels ran down much faster in inside-out single-channel patches than in macropatches after extended perfusion.

Whole-cell current was measured by TEVC with the OC-725C oocyte clamp amplifier (Warner Instruments). Recording glass electrodes filled with 3 M KCl had a resistance of 0.2–1 MΩ. The external solution contained 90 mM KCl, 3 mM $MgCl_2$, and 10 mM HEPES (pH 7.3 with KOH) and was perfused by gravity at a speed of ~1 ml/min through a chamber with a volume of ~100 μl.

Data acquisition and analysis were performed with a customized program written in Axobasic language (Axon Instruments) on a 586 PC through a Digidata 1200 interface. Currents were elicited at an interval of 1–10 s by voltage ramps from −100 mV (or, in a few cases, −200 mV) to +80 mV over 70–200 ms, from a holding potential of −40 or 0 mV. In macropatch recordings, current records were filtered at 4 kHz and digitized at 10 kHz. In single-channel recordings, we took advantage of the long open and closed times of the single Kir2.1 channel, filtering current records at 100 Hz and sampling data at 2.5 kHz. In some experiments, we also filtered the single-channel records at 1 kHz and did not observe a significant increase in the open-channel noise (relative to the baseline). Experiments were done at room temperature (22°C–24°C).

MTS reagents (Toronto Research Chemicals) and qBBr (Molecular Probes) were stored at −20°C and were dissolved in bath solution prior to each experiment, generally $<$1 min before application. MTSEA (2.5 mM), MTSET (2 mM), MTS-PTrEA (2 mM), or qBBr (4 mM) was applied for 2–8 min until modification reached a steady state. The effect of a reagent was calculated from the current amplitude measured at −80 mV, obtained before application and after washout of the reagent. No corrections were made for leakage current or for current rundown, which were negligible in macropatch recordings. The time constant of modification was obtained by fitting the time course with a single exponential. The apparent second-order rate constant of MTSEA and MTSET reactions with the cysteine mutant channels was then calculated as the reciprocal of the time constant divided by the concentration. Data are presented as mean ± SD (number of observations). The statistical test was performed with a Student's t test.

Acknowledgments

We thank Dr. Arthur Karlin for insightful discussions and the suggestion to use qBBr. We also thank Yong Gang Zhu for excellent technical assistance with molecular biology. J. Y. is an Alfred P. Sloan Fellow. This work was supported by a National Institutes of Health research grant.

Received October 19, 1998; revised January 29, 1999.

References

Adrian, R.H. (1969). Rectification in muscle membrane. Prog. Biophys. Mol. Biol. *19*, 340–369.

Akabas, M.H., Stauffer, D.A., Xu, M., and Karlin, A. (1992). Acetylcholine receptor channel structure probed in cysteine-substitution mutants. Science *258*, 307–310.

Chen, X.H., Bezprozvanny, I., and Tsien, R.W. (1996). Molecular basis of proton block of L-type Ca^{2+} channels. J. Gen. Physiol. *108*, 363–374.

Doyle, D.A., Cabral, J.M., Pfuetzner, R.A., Kuo, A., Gulbis, J.M., Cohen, S.L., Chait, B.T., and MacKinnon, R. (1998). The structure of the potassium channel: molecular basis of K^+ conduction and selectivity. Science *280*, 69–77.

Fakler, B., Brandle, U., Glowatzki, E., Weidemann, S., Zenner, H.-P., and Ruppersberg, J.P. (1995). Strong voltage-dependent inward rectification of inward rectifier K^+ channels is caused by intracellular spermine. Cell *80*, 149–154.

Ficker, E., Taglialatela, M., Wible, B.A., Henley, C.M., and Brown, A.M. (1994). Spermine and spermidine as gating molecules for inward rectifier K^+ channels. Science *266*, 1068–1072.

Glowatzki, E., Fakler, G., Brandle, U., Rexhausen, U., Zenner, H.P., Ruppersberg, J.P., and Fakler, B. (1995). Subunit-dependent assembly of inward-rectifier K^+ channels. Proc. R. Soc. Lond. B Biol. Sci. *261*, 251–261.

Hagiwara, S., and Jaffe, L.A. (1979). Electrical properties of egg cell membranes. Annu. Rev. Biophys. Bioeng. *8*, 385–416.

Hagiwara, S., Miyazaki, S., and Rosenthal, N.P. (1976). Potassium current and the effect of cesium on this current during anomalous rectification of the egg cell membrane of a starfish. J. Gen. Physiol. *67*, 621–638.

Hille, B. (1992). Ionic Channels of Excitable Membranes (Sutherland, Massachusetts: Sinauer Associates).

Hille, B., and Schwarz, W. (1978). Potassium channels as multiion pores. J. Gen. Physiol. *72*, 409–442.

Ho, K., Nichols, C.G., Lederer, W.J., Lytton, J., Vassilev, P.M., Kanazirska, M.V., and Hebert, S.C. (1993). Cloning and expression of an inwardly rectifying ATP-regulated potassium channel. Nature *362*, 31–38.

Holmgren, M., Smith, P. L., and Yellen, G. (1997). Trapping of organic blockers by closing of voltage-dependent K^+ channels: evidence for a trap door mechanism of activation gating. J. Gen. Physiol. *109*, 527–535.

Isacoff, E.Y., Jan, Y.N., and Jan, L.Y. (1991). Putative receptor for the cytoplasmic inactivation gate in the *Shaker* K^+ channel. Nature *353*, 86–90.

Ishihara, K., Mitsuiye, T., Noma, A., and Takano, M. (1989). The Mg^{2+}-block and intrinsic gating underlying inward rectification of the K^+ current in guinea-pig cardiac myocytes. J. Physiol. *419*, 297–320.

Jan, L.Y., and Jan, Y.N. (1997). Voltage-gated and inwardly rectifying potassium channels. J. Physiol. *505*, 267–282.

Jordan, P.C. (1982). Electrostatic modeling of ion pores: energy barriers and electric field profiles. Biophys. J. *39*, 157–164.

Karlin, A., and Akabas, M.H. (1998). Substituted-cysteine accessibility method. Methods Enzymol. *293*, 123–145.

Kosower, N.S., Kosower, E.M., Newton, G.L., and Ranney, H.M. (1979). Bimane fluorescent labels: labeling of normal human red cells under physiological conditions. Proc. Natl. Acad. Sci. USA *76*, 3382–3386.

Kubo, Y., Baldwin, T.J., Jan, Y.N., and Jan, L.Y. (1993). Primary structure and functional expression of a mouse inward rectifier potassium channel. Nature *362*, 127–133.

Levitt, D.G. (1978). Electrostatic calculations for an ion channel. I. Energy and potential profiles and interactions between ions. Biophys. J. *22*, 209–219.

Liman, E.R., Tytgat, J., and Hess, P. (1992). Subunit stoichiometry of a mammalian K^+ channel determined by construction of multimeric cDNAs. Neuron *9*, 861–871.

Liu, Y., Holmgren, M., Jurman, M.E., and Yellen, G. (1997). Gated access of the pore of a voltage-dependent K^+ channel. Neuron *19*, 175–184.

Lopatin, A.N., Makhina, E.N., and Nichols, C.G. (1994). Potassium channel block by cytoplasmic polyamines as the mechanism of intrinsic rectification. Nature *372*, 366–369.

Lopatin, A.N., Makhina, E.N., and Nichols, C.G. (1995). The mechanism of inward rectification of potassium channels: "long-pore plugging" by cytoplasmic polyamines. J. Gen. Physiol. *106*, 923–955.

Lu, Z., and MacKinnon, R. (1994). Electrostatic tuning of Mg^{2+} affinity in an inward-rectifier K^+ channel. Nature *371*, 243–246.

MacKinnon, R. (1994). Determination of the subunit stoichiometry of a voltage-activated potassium channel. Nature *350*, 232–235.

Matsuda, H. (1988). Open-state substructure of inwardly rectifying potassium channels revealed by magnesium block in guinea-pig heart cells. J. Physiol. *397*, 237–258.

Matsuda, H., Saigusa, A., and Irisawa, H. (1987). Ohmic conductance through the inwardly rectifying K channel and blocking by internal Mg^{2+}. Nature *325*, 156–158.

Nichols, C.G., Ho, K., and Hebert, S. (1994). Mg^{2+}-dependent inward rectification of ROMK1 potassium channels expressed in Xenopus oocytes. J. Physiol. *476*, 399–409.

Oishi, K., Omori, K., Ohyama, H., Shingu, K., and Matsuda, H. (1998). Neutralization of aspartate residues in the murine inwardly rectifying K^+ channel IRK1 affects the substate behaviour in Mg^{2+} block. J. Physiol. *510*, 675–683.

Oliver, D., Hahn, H., Antz, C., Ruppersberg, J.P., and Fakler, B. (1998). Interaction of permeant and blocking ions in cloned inward-rectifier K^+ channels. Biophys. J. *74*, 2318–2326.

Omori, K., Oishi, K., and Matsuda, H. (1997). Inwardly rectifying potassium channels expressed by gene transfection into the Green Monkey kidney cell line COS-1. J. Physiol. *499*, 369–378.

Root, M.J., and MacKinnon, R. (1994). Two identical noninteracting sites in an ion channel revealed by proton transfer. Science *265*, 1852–1856.

Silver, M.R., and DeCoursey, T.E. (1990). Intrinsic gating of inward rectifier in bovine pulmonary artery endothelial cells in the presence or absence of internal Mg^{2+}. J. Gen. Physiol. *96*, 109–133.

Spassova, M., and Lu, Z. (1998). Coupled ion movement underlies rectification in an inward-rectifier K^+ channel. J. Gen. Physiol. *112*, 211–221.

Stanfield, P.R., Davies, N.W., Shelton, P.A., Sutcliffe, M.J., Khan, I.A., Brammar, W.J., and Conley, E.C.J. (1994). A single aspartate residue is involved in both intrinsic gating and blockage by Mg^{2+} of the inward rectifier, IRK1. J. Physiol. *478*, 1–6.

Stauffer, D.A., and Karlin, A. (1994). Electrostatic potential of the acetylcholine binding sites in the nicotinic receptor probed by reactions of binding-site cysteines with charged methanethiosulfonates. Biochemistry *33*, 6840–6849.

Taglialatela, M., Wible, B.A., Caporaso, R., and Brown, A.M. (1994). Specification of pore properties by the carboxyl terminus of inwardly rectifying K^+ channels. Science *264*, 844–847.

Taglialatela, M., Ficker, E., Wible, B.A., and Brown, A.M. (1995). C-terminus determinants for Mg^{2+} and polyamine block of the inward rectifier K^+ channel IRK1. EMBO J. *14*, 5532–5541.

Vandenberg, C.A. (1987). Inward rectification of a potassium channel in cardiac ventricular cells depends on internal magnesium ions. Proc. Natl. Acad. Sci. USA *84*, 2560–2564.

Yang, J., Jan, Y.N., and Jan, L.Y. (1995a). Control of rectification and permeation by residues in two distinct domains in an inward rectifier K^+ channel. Neuron *14*, 1047–1054.

Yang, J., Jan, Y.N., and Jan, L.Y. (1995b). Determination of the subunit stoichiometry of an inwardly rectifying potassium channel. Neuron *15*, 1441–1447.